Journal of Power Sources 196 (2011) 10717–10726

Contents lists available at SciVerse ScienceDirect

Journal of Power Sources

journal homepage: www.elsevier.com/locate/jpowsour

Intelligent electric vehicle charging: Rethinking the valley-fill

Keenan Valentine, William G. Temple, K. Max Zhang *

Sibley School of Mechanical and Aerospace Engineering, Cornell University, Ithaca, NY 14853, United States

ARTICLE INFO

Article history:
Received 10 June 2011
Received in revised form 17 August 2011
Accepted 18 August 2011
Available online 25 August 2011

Keywords:
Smart grid
Demand-side management
Electricity markets
Generator ramping
Charging constraint
Driving pattern

ABSTRACT

This study proposes an intelligent PEV charging scheme that significantly reduces power system cost while maintaining reliability compared to the widely discussed valley-fill method of aggregated charging in the early morning. This study considers optimal PEV integration into the New York Independent System Operator's (NYISO) day-ahead and real-time wholesale energy markets for 21 days in June, July, and August of 2006, a record-setting summer for peak load. NYISO market and load data is used to develop a statistical Locational Marginal Price (LMP) and wholesale energy cost model. This model considers the high cost of ramping generators at peak-load and the traditional cost of steady-state operation, resulting in a framework with two competing cost objectives. Results show that intelligent charging assigns roughly 80% of PEV load to valley hours to take advantage of low steady-state cost, while placing the remaining 20% equally at shoulder and peak hours to reduce ramping cost. Compared to unregulated PEV charging, intelligent charging reduces system cost by 5–16%; a 4–9% improvement over the flat valley-fill approach. Moreover, a Charge Flexibility Constraint (CFC), independent of market modeling, is constructed from a vehicle-at-home profile and the mixture of Level 1 and Level 2 charging infrastructure. The CFC is found to severely restrict the ability to charge vehicles during the morning load valley. This study further shows that adding more Level 2 chargers without regulating PEV charging will significantly increase wholesale energy cost. Utilizing the proposed intelligent PEV charging method, there is a noticeable reduction in system cost if the penetration of Level 2 chargers is increased from 70/30 to 50/50 (Level 1/Level 2). However, the system benefit is drastically diminished for higher penetrations of Level 2 chargers.

1. Introduction

There is an increasing need for flexible loads that can respond to economic and reliability signals from energy providers to decrease energy cost and enhance the security of the grid [1,2]. This dispatchable demand – much like generation – can be monitored and controlled by energy aggregators, such as ISOs/RTOs and utilities, to maintain generation and load balance via load scheduling, shifting, curtailing and provision of ancillary services [3,4]. Load services can lower Locational Marginal Prices (LMPs), ease incorporation of intermittent renewable energy, and lower pollutant emissions from generators such as CO_2, NO_x, and SO_2 [2,5]. Since a majority of the capital costs of acquiring flexible loads are covered by the customer for their primary functionalities (e.g. electric vehicles for transportation), energy aggregators will be tasked to provide the remaining monitor and control technology to network individual customers and energy providers.

The charging of lithium-ion batteries in Plug-in Electric Vehicles (PEVs) is one type of dispatchable load that has significant potential to provide many types of power system services without causing customer discomfort [3]. The control of PEV charging will most likely involve discontinuous and/or variable charging of individual vehicles, which studies show does not cause battery degradation [6,7]. As 85% of commuters in the U.S. drive 40 miles or less every day, the charging need for a typical PEV-40 (40-mile electric range) ranges from 10 kWh for a compact sedan to 18.4 kWh for a full-size sports utility vehicle (SUV) [8]. In this study, Level 1 chargers deliver 1.44 kW and Level 2 chargers deliver 7.68 kW in a typical household [9]. Level 2 chargers with higher power ratings are not analyzed as it may cause current batteries and distribution transformers to overheat during vehicle charging. Furthermore, PEVs will most likely be charged at owner's homes, at least in the short-term [10]. Consensus shows that unregulated charging of PEVs – allowing commuters to charge after work in the evening – will increase peak-load and LMP, while decreasing system reliability [10–12]. To prevent these undesirable consequences current literature suggests several regulated charging solutions, most notably the valley-fill scheme, where all charging takes place during the early morning, when system power demand is lowest [11,13].

* Corresponding author.
E-mail address: kz33@cornell.edu (K.M. Zhang).

0378-7753/$ – see front matter © 2011 Elsevier B.V. All rights reserved.
doi:10.1016/j.jpowsour.2011.08.076

Table 1
Summary of PEV charging methods.

Charging method	Description
Unregulated	Charging begins immediately after a commuter returns home from work, incurring the highest cost.
Flat valley-fill	Charging is regulated to take place when system demand is lowest, incurring the lowest steady-state cost.
Smooth valley-fill	A valley-fill variation with minor smoothing at the endpoints of the valley to reduce ramping cost.
Intelligent	Charging can be dispatched whenever commuters are at home to minimize total system cost from steady-state and ramping operation.

This study examines the maximum aggregated potential of PEV load to minimize a two-settlement wholesale energy market cost (system cost) and investigates the associated optimal scheduling of dispatchable PEV load in the New York Control Area (NYCA) – the power system in New York State. The New York Independent System Operator (NYISO) oversees NYCA along with parts of the Canadian system. NYCA interconnects PJM, New England, Ontario and Hydro Quebec. NYCA has a Total Resource Requirement of nearly 39,000 MW with 63% of capacity from gas and oil units, 14% from nuclear, 11% from hydro and 7% from coal.

This study considers zero capital, operation, and maintenance cost for PEV load services so as to determine the system value of controlling PEV charging.

2. Electric vehicle load and traditional charging methods

Understanding the impact of electric vehicle charging on the power system requires characterizing both the number of vehicles and the time-dependant charging distribution. In this study, electric vehicle energy demand is characterized from US Census data, and two well known charging patterns – unregulated charging and valley-filling – are discussed. Table 1 presents a summary of all charging strategies outlined in the following sections (intelligent charging is discussed in Section 5).

2.1. Energy requirement modeling

Prior to investigating different PEV charging schedules, the total energy requirement of vehicle fleet must be determined. PEV charging in New York State is studied. The total number of vehicles within the state, approximated as the total number of commuters who drive to their place of work, is 4.6 million. This study obtained commuter data from the 2000 Census [14]. Once the number of vehicles is known, various PEV market penetration percentages are applied to obtain the number of PEVs on the road for a penetration level.

This study partitions the NYCA into 19 load centers detailed in the 36-bus Northeast Power Coordinating Council (NPCC) power system reduction model [15]. Population density data from the 2000 Census were used to apply “center city”, “suburban”, and “rural” labels to each of the 19 load centers in NYCA. To obtain the total PEV energy requirement in New York, the number of vehicles is multiplied by a distance driven daily, and any distance that is less than or equal to 40 miles is in turn translated to a PEV charge energy requirement. Liquid fuel is assumed to power PEVs above the 40 miles mark. Driving distances were computed using US Department of Energy data, specifying the average distance driven in “rural”, “suburban”, and “center city” regions. The average distances are 59.4 km (or 36.9 miles), 46.3 km (or 28.8 miles) and 43.8 km (or 27.2 miles), respectively [16].

For each load center, a weighted average rate derived from 0.16 kWh km^{-1} (or 0.25 kWh mile^{-1}) for compact sedans to 0.29 kWh km^{-1} (or 0.46 kWh mile^{-1}) for SUVs is applied to convert miles driven to energy usage [8]. Eq. (1) describes the required energy.

$$\text{Daily PEV energy} = \sum_{i=1}^{19} M_{\text{PEV}} N_i D_i E_i \tag{1}$$

where M_{PEV} is the PEV market penetration and N_i, D_i, E_i are the number of commuting vehicles, average daily distance driven and the average electric energy used per mile at load center i, respectively. In terms of energy contribution, 5%, 10%, 20%, and 40% penetrations of PEVs charging between the valley-load hours of 3 AM to 6 AM is on average 2.6%, 5.3%, 10.6%, 21.1% of summertime electricity consumption during the same time frame.

2.2. Unregulated charging model

Unregulated charging refers to a method that charges the PEVs as soon as the commuter arrives home, and finishes charging when the battery becomes full or when the commuter leaves home. This type of charging scheme tends to exacerbate peak load and LMP.

The power consumption model for unregulated charging is largely the same as that in [12]. In summary, the charging scheme assumes that commuters start their commute from home with a fully charged battery. The time-varying electricity demand from PEVs is simulated using the number of commuters, PEV market penetrations, the times when commuters leave work, the speeds at which they travel, the daily commuting distances and the charger power ratings (Level 1 or Level 2). These input parameters were synthesized from the Regional Travel Household Interview Survey (RTHIS) and the 2000 Census Transportation Planning Package (CTPP).

In addition to these parameters, a traffic congestion factor known as Travel Time Index (TTI) of 1.15 is used in the Monte Carlo simulation of a thousand commuters to create a normalized commuter-at-home profile (CHP) and an unregulated charging profile [17–19]. The simulation provides a realistic sample of a variety of commuter transportation patterns that include different battery recharge requirements, home arrival and departure times. The CHP and unregulated charging profile is shown in Fig. 1.

The normalized CHP has a sinusoidal shape whose valley is at 7:30 AM and peak at 7 PM, with peak approximately 7 times the valley. The normalized unregulated charging profile has a more skewed sinusoidal shape whose valley is at 6:30 AM and peak at 6 PM with peak about 15 times the valley. The unregulated charging profile is phased approximately 1–2 h ahead of the CHP. This is because the CHP is the number of commuters at home, not the number of commuters arriving home. Consequently, many of the

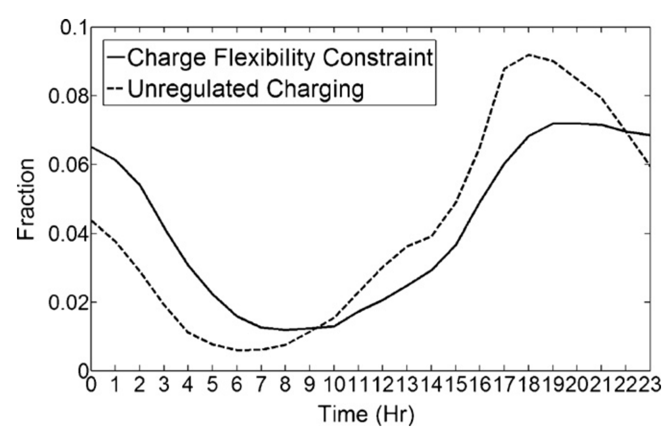

Fig. 1. Normalized Charging Flexibility Constraint (CFC) and unregulated PEV charging profile.

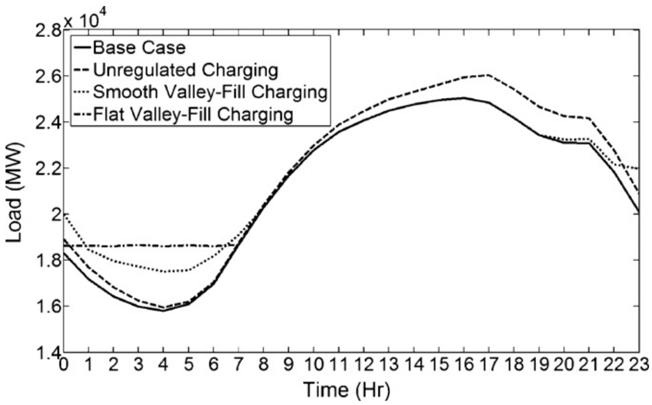

Fig. 2. Base case load profile with unregulated, smooth and flat valley-fill charging schemes for 40% PEV penetration.

commuters that arrive home before 7 PM have finished charging their PEV batteries by 7 PM. A similar phenomenon occurs in the morning.

2.3. Valley-fill charging model

Valley-filling is an approach that intuitively allocates all of PEVs' required charge at valley-load hours. This approach only charges PEVs at lowest steady-state loads and LMPs. The traditional valley-fill approach allocates PEV charge such that certain hours of the valley achieve a flat load. There are several variations on this basic approach, including minor smoothing for generator ramping reduction (see Section 3). Examples of previously analyzed PEV charging schemes are depicted in Fig. 2.

3. Wholesale energy market model

The New York Independent System Operator (NYISO) operates on a two-settlement energy market: day-ahead and real-time. Traditionally, Locational Marginal Prices (LMPs) and wholesale energy cost are determined from the unit commitment of generators in the day-ahead market (DAM) and economic dispatch in the real-time market (RTM), while observing security constraints and emissions permits [20]. As generator offer curves, transmission network topology, network security constraints, and generator emission profiles are proprietary, this study develops an alternative statistical approach for assessing market cost for the entire NYCA using historical market and operation data. Consequently, the model approximates the LMP and system cost changes due to PEV penetrations in the NYCA without explicitly employing the techniques of unit commitment and economic dispatch. Principally, the model incorporates the entire generation fleet in the NYCA; therefore it does not couple PEV charging to a specific generator [4]. As a result, the dispatch of PEV charging provides direct benefit to the entire power system in NYCA.

This model expands the traditional steady-state dispatch model to explicitly include the system cost of ramping generators. The traditional steady-state cost model depends on the load at a dispatch time, and is constrained only by physical generator ramp rates without explicit cost assignment. However, it is evident that generators incur higher cost (maintenance and fuel consumption) when rapidly changing their set-points to match load changes [21]. This additional cost is the ramping cost. It is likely that this cost will become more significant as the power system incorporates a larger share of intermittent generation [22].

3.1. Power system data

The NYISO provides an extensive archive of historical day-ahead and real-time load and LMP data. As the highest system loads occur in the summertime, this study considers only the summer months from June to August in order to characterize the maximum system benefit of intelligent PEV charging. The data used for this study consists of 21 days from the summer of 2006: June 19–25, July 9–15, and August 13–19. The year 2006 was chosen for its record-setting summer peak loads. These 21 days were also selected to provide a thorough characterization of the time-varying nature of summer loads and LMPs.

3.2. System cost

The system cost for the energy market is formulated as the sum of the DAM cost and cost of *dispatch adjustment* from the RTM, where cost is the product of LMP and load served by generators. This relationship is given in Eq. (2).

$$\text{Daily total system cost} = \sum_{t=0}^{T_1} \text{LMP}_{\text{DAM},t}(P_{\text{DAM},t}|\Delta P_{\text{DAM},t}|) \times P_{\text{DAM},t} + \sum_{t=0}^{T_2} \text{LMP}_{\text{RTM},t}(P_{\text{RTM},t}, |\Delta P_{\text{RMT},t}|) \times (P_{\text{RMT},t} - P_{\text{DAM},t}) \qquad (2)$$

where the subscripts DAM and RTM refer to the day-ahead and real-time markets, respectively. LMP at time t is a function of steady-state load, P, and modulus of load difference, $|\Delta P|$ (assuming a symmetric ramping cost). T_1 is the 23rd hour in the DAM and T_2 is the 143rd 10-min period in the RTM. The first summation in Eq. (2) is DAM cost and the second summation is the cost of RTM adjustment to DAM.

3.3. LMP model

This study incorporates a statistical LMP model for NYCA with PEV charge allocation affecting the LMP. The model uses base case LMPs from the 2006 summer to establish a 0% PEV penetration base case.

3.3.1. Cost model: inter-day

To capture the LMP trend of the summer season from the 21 selected days and to ensure accuracy from the use of Taylor Series expansion around the base case loads and LMPs, weighted average values of base case load, modulus of ramp and LMP were used to construct an approximate model for the daily system cost. This averaging method also preserves the sensitivity of system cost due to load changes while dampening the instability of real-time prices (see Section 3.3.2.).

Eq. (3) shows the averaging process, while Eq. (4) re-expresses Eq. (2) in terms of averaged variables.

$$\sum_{t \in T} \text{LMP}_t(P_t, |\Delta P_t|) \times P_t \approx \overline{\text{LMP}}(\bar{P}, \overline{|\Delta P|}) \times \bar{P}_{\text{sys}} \qquad (3)$$

where weighted averaging is indicated by the accent bar and $\bar{P}_{\text{sys}}$ is the equivalent average system load at time t (see Section 3.3.2.).

$$\text{Daily total system cost} \approx \overline{\text{LMP}}_{\text{DAM}}(\bar{P}_{\text{DAM}}, \overline{|\Delta P_{\text{DAM}}|}) \times \bar{P}_{\text{sys,DAM}} + \overline{\text{LMP}}_{\text{RTM}}(\bar{P}_{\text{RTM}}, \overline{|\Delta P_{\text{RTM}}|}) \times (\bar{P}_{\text{sys,RTM}} - \bar{P}_{\text{sys,DAM}}) \qquad (4)$$

Table 2
Comparison of the average LMP model used to the Simple Regression Model and MATPOWER.

LMP ratio	New York state		Northeast Power Coordinating Council	
	Simple Regression Model	Avg. LMP model	MATPOWER	Avg. LMP model
Unregulated/base case	1.071	1.051	1.029	1.022
Valley-fill/base case	1.027	0.982	N/A	N/A
Unregulated/valley-fill	1.043	1.070	N/A	N/A

Taylor series expansion of the average LMP function around the base case results in Eq. (5):

$$\overline{\mathrm{LPM}}(\bar{P},\overline{|\Delta P|}) \approx a_0 + a_1\bar{P} + a_2\bar{P}^2 + a_3\bar{P}\overline{|\Delta P|} + a_4\overline{|\Delta P|} + a_5\overline{|\Delta P|}^2 \quad (5)$$

where a_i is a constant.

Principle component analysis was performed to assess the magnitude of the terms in Eq. (5), showing negligible $\overline{|\Delta P|}$ and $\overline{|\Delta P|}^2$ contribution. The final form of the average LMP equation is given in Eq. (6):

$$\overline{\mathrm{LPM}}(\bar{P},\overline{|\Delta P|} \approx a_0 + a_1\bar{P} + a_2\bar{P}^2 + a_3\bar{P}\overline{|\Delta P|}) \quad (6)$$

Eq. (6) statistically demonstrates that average NYCA LMP can be approximated by a quadratic function of average load, $\bar{P}$, with a ramping term, $\bar{P}\overline{|\Delta P|}$. The constants in this expression were determined from least-squares regression of NYISO DAM and RTM LMP and load data for the 21 summer days.

Physically, Eq. (6) shows that system ramping is more costly at peak-load than at valley-load due to the use of expensive peaking units.

3.3.2. *Weighted average load: intra-day*

Within a given day, the model must reflect the high cost of adding load at peak. Therefore, the average system load is a weighted average of three load regions: peak, shoulder and valley. Peak and valley-load hours account for approximately 12 h in each day, so the sum of the peak-load weight (W_p) and the valley-load weight (W_v) adds up to ½. C_p and C_v are user-defined tuning factors that allow adjustment of the average LMP model to match market data. Thus,

$$C_pW_p + C_vW_v = \frac{1}{2} \quad (7)$$

Letting $R = W_p/W_v$ and $S = c_p/c_v$,

$$C_pW_p = \frac{RS}{2(1+RS)} \quad \text{and} \quad C_vW_v = \frac{1}{2(1+RS)} \quad (8)$$

In model implementation, R is calculated from the ratio of peak-load to valley-load and S is defined in the interval $[1/R \le S \le 3/R]$. For example, a value of $S = 1/R$ results in $C_pW_p = C_vW_v = 1/4$: the non-weighted average load. A value of $S = 1$ was chosen for the average LMP model to approximate the NYCA load and LMP data. It is worth noting that S can be adjusted to better fit data from other control areas.

Finally, the weighted-average load is obtained from Eq. (9):

$$\bar{P} = \sum_{i=1}^{I_1} C_pW_pP_{p,i} + \sum_{i=1}^{I_2} C_vW_vP_{v,i} + \sum_{i=1}^{12}\frac{1}{2}P_{s,i} \quad (9)$$

where P is load from data, s is shoulder-load region, and $I_1 + I_2 = 12$.

The equivalent system load, $\bar{P}_{sys}$, is a also function of both $\bar{P}$ and $\overline{|\Delta P|}$, as is in the case with LMP.

$$\bar{P}_{sys} = \bar{P}_{sys}(\bar{P},\overline{|\Delta P|}) \quad (10)$$

Taylor series is employed to linearize $\bar{P}_{sys}$, resulting in Eq. (11).

$$\bar{P}_{sys} \approx b_0 + b_1\bar{P} + b_2\overline{\Delta P} \quad (11)$$

The constants, b_i, are determined from fitting the ratio of system cost of unregulated PEV charge scheme to the base case such that it approximates the costs from the validation models in Section 3.3.3. For the NYCA, $b_0 \approx 0$, $b_1 \approx 1$ and $b_2 \approx 1$. Consequently the final expression for $\bar{P}_{sys}$ is given in Eq. (12),

$$\bar{P}_{sys} \approx \bar{P} + \overline{|\Delta P|} \quad (12)$$

It is worth noting that the coefficients in Eqs. (6) and (11) can be tuned to analyze different scenarios of system ramping on wholesale energy cost, such as from incorporating volatile generation.

3.3.3. *Model verification and validation*

The average LMP model was checked for accuracy and stability across various load and PEV charging patterns. Specifically, four sample load curves (pictured in Fig. 2) with 40% PEV penetration were tested: first is a base case without PEV charging, second is with a flat valley-fill charge, third is with a smoothed valley-fill charge (which adheres to the charging constraint), and last is with an unregulated PEV charge profile.

Two reference models were used to validate the performance of the average LMP model for these four load curves. The first reference model is a simple load-only regression model, where a quadratic curve is regressed to the base case load and LMP data.

The second reference model uses MATPOWER, a security-constrained optimal power flow analysis tool, paired with the 36-bus reduced NPCC network, which includes New York, New England, and parts of Pennsylvania and Canada [15,23]. MATPOWER was used to run economic dispatch of 693 generators in the reduced NPCC network for the base case as well as the unregulated charging case with PEV load scaled up from the NYCA base case to match the NPCC base case. Network constraints were disabled to produce purely economic dispatch prices for comparison with the average LMP with ramp model. The valley-fill case was not considered for economic dispatch, because MATPOWER currently uses a myopic optimization method that is not suited for non-linear ramp costs related to the valley-fill method.

Table 2 shows comparative results among the three LMP models average for the 21 summer days. The results are tabulated as ratios of different PEV charging scenarios and the base case. The smooth valley-fill and the flat valley-fill obtained close results, therefore only the smooth valley-fill results are shown. For the Simple Regression Model comparison the PEV market penetration is 40%; for the MATPOWER model the market penetration is 20%.

Table 2 validates the results of the average LMP model, showing variations ranging from 0.7% for the MATPOWER comparison, to 4.4% for the Simple Regression Model comparison. Interestingly, the average LMP model has a price ratio less than 1 for the valley-fill to base case comparison. This is due to additional load from PEV charging that smoothes the load curve reducing system ramping cost.

4. Charge Flexibility Constraint

The Charge Flexibility Constraint (CFC) is a function of commuter driving patterns and the charging infrastructure deployed throughout the system which limits the power withdraw. In this analysis, it

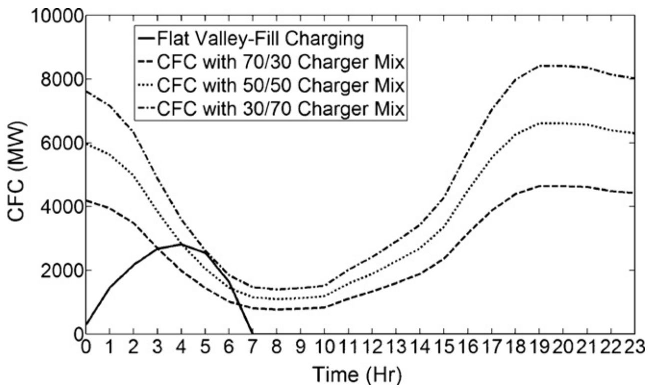

Fig. 3. Flat valley-fill PEV charging profile overlaid with Charge Flexibility Constraint (CFC) for 70/30, 50/50 and 30/70 (Level 1/Level 2) charging infrastructure.

is assumed that PEV charging only takes place at the vehicle owners' homes, resulting in the CHP (see Section 2.2). If charging is allowed to take place at other locations, such as at work, then a less restrictive profile describing vehicle idleness would be used instead.

The type of charging station available to an individual imposes an additional limitation on power consumption. There are two types of electric vehicle chargers considered in this study: Level 1 chargers are standard 120 V/12 A outlets, capable of delivering a maximum of 1.44 kW, while Level 2 chargers considered in this study are rated at 240 V/32 A and can deliver 7.68 kW (see Introduction for rationale) [9].

The aggregate PEV charging constraint for a specified time period, expressed in kilowatts, is given by Eq. (13):

$$\mathrm{CFC}(t) \le \mathrm{CHP}(t) M_{\mathrm{PEV}} N[1.44\alpha + 7.68(1-\alpha)] \tag{13}$$

where M_{PEV} is the market penetration of PEVs, N is the total number of vehicle owners, and α is the fraction of Level 1 vehicle chargers.

The CFC is independent of any wholesale market model, and is enforced for all PEV charging schemes. Fig. 3 shows that at valley-load hours, the maximum charging power decreases sharply from 1 AM to 6 AM averaging close to 1 GW h^{-1}. From 6 AM to 8 AM the CFC achieves its minimum at approximately 700 MW for a 70/30 Level 1/Level 2 charger mixture.

Fig. 3 shows that a flat valley-fill charging scheme violates the CFC for a 70/30 charger mix. It is worth noting that the 70/30 ratio corresponds to an average 3.31 kW power draw for each vehicle, and most PEVs on the road today (Chevy Volt and Nissan Leaf) are limited by the onboard power converter to 3.3 kW. To accommodate the possibility of a flat valley-fill charging scheme, significant infrastructure investment must be made to attain a 30/70 charger mixture. The system benefit of such an investment is further discussed in Section 6.4.

5. Intelligent PEV charging

Intelligent Charging allows an aggregator to allocate PEV charging such that overall system steady-state and ramping costs are minimized in the day-ahead and real-time wholesale energy markets. Intelligent charging also considers the realistic aggregate charging constraint imposed by the CFC. This charging scheme can occur at any time when commuters are at home, and is therefore not limited to valley-load hours. Mathematically, intelligent charging changes system load profiles and ramping requirements such that both $\bar{P}$ and $\overline{|\Delta P|}$ change.

Total system cost was determined through a linked two-stage optimization process, which was solved for each of the 21 days using Simulated Annealing, a metaheuristic that has been successfully applied to many problems in power systems [24–26]. For each day, the optimization problem is formulated in Eqs. (14)–(18) for the DAM stage and Eqs. (19)–(21) for the RTM stage.

Day-ahead market stage

$$\min_{\mathrm{PEV}_{\mathrm{DAM},t},\mathrm{PEV}_{\mathrm{RTM},t}} \left\{\overline{\mathrm{LPM}}_{\mathrm{DAM}}(\bar{P}_{\mathrm{DAM}}, \overline{|\Delta P_{\mathrm{DAM}}|}) \times \bar{P}_{\mathrm{sys,DAM}} + E[\overline{\mathrm{LPM}}_{\mathrm{RTM}}(\bar{P}_{\mathrm{RTM}}, \overline{|\Delta P_{\mathrm{RTM}}|}) \times (\bar{P}_{\mathrm{sys,RTM}} - \bar{P}_{\mathrm{sys,DAM}})]\right\} \tag{14}$$

s.t.

$$0 \le \mathrm{PEV}_{\mathrm{DAM},t} \le \mathrm{CFC}_t \quad \forall t \in \{0, \ldots, T_1\} \tag{16}$$

$$0 \le \mathrm{PEV}_{\mathrm{RTM},t} \le \mathrm{CFC}_t \quad \forall t \in (0, \ldots, T_1) \tag{15}$$

$$0 \le \sum_{t=0}^{T_1} \mathrm{PEV}_{\mathrm{DAM},t} \le \sum_{i=1}^{19} M_{\mathrm{PEV}} N_i D_i E_i \tag{17}$$

$$\sum_{t=0}^{T_1} \mathrm{PEV}_{\mathrm{RTM},t} = \sum_{i=1}^{19} M_{\mathrm{PEV}} N_i D_i E_i \tag{18}$$

Real-time market stage

$$\min_{\mathrm{PEV}_{\mathrm{RTM},t}} \left\{\overline{\mathrm{LPM}}_{\mathrm{DAM}}(\bar{P}_{\mathrm{DAM}}, \overline{|\Delta P_{\mathrm{DAM}}|}) \times \bar{P}_{\mathrm{sys,DAM}} + [\overline{\mathrm{LPM}}_{\mathrm{RTM}}(\bar{P}_{\mathrm{RTM}}, \overline{|\Delta P_{\mathrm{RTM}}|}) \times (\bar{P}_{\mathrm{sys,RTM}} - \bar{P}_{\mathrm{sys,DAM}})]\right\} \tag{19}$$

$$0 \le \mathrm{PEV}_{\mathrm{RTM},t} \le \mathrm{CFC}_t \quad \forall t \in \{0, \ldots, T_2\} \tag{20}$$

$$\sum_{t=0}^{T_2} \mathrm{PEV}_{\mathrm{RTM},t} = \sum_{i=1}^{19} M_{\mathrm{PEV}} N_i D_i E_i \tag{21}$$

where for each day, $\mathrm{PEV}_{\mathrm{DAM},t}$ and $\mathrm{PEV}_{\mathrm{RTM},t}$ are the PEV charging committed in the day-ahead market (DAM) and dispatched in the real-time market (RTM), respectively.

The DAM solver uses NYISO day-ahead load forecasts for the base load, and the unregulated charging case profile as the initial solution to minimize the energy market cost given a daily PEV energy requirement. The day-ahead solver has an expectation of the RTM LMP based on historical data to evaluate the cost effectiveness of *hourly* PEV charge allocation in the DAM. Moreover, the daily PEV energy requirement is an inequality constraint in the DAM (Eq. (17)), and an equality constraint in the expected RTM (Eq. (18)). This way PEVs are guaranteed charging without forcing day-ahead commitment. At this stage, the PEV charge allocation in the DAM is binding, and that in the expected RTM is not binding. The second RTM stage in the optimization algorithm solves for the actual real-time PEV allocation, *in 10-min increments*, given the predetermined day-ahead schedule in the first DAM stage. The second stage uses the same LMP model, but with coefficients regressed for the real-time market. The PEV energy requirement is active in this RTM stage (Eq. (21)).

6. Results and discussion

6.1. Load profiles with intelligently charged PEVs

Fig. 4 shows typical intelligent charging allocations for the 21 summer days tested. Results indicated that charging mostly occurs during 7 valley-load hours of 1 AM to 8 AM. However, there is noticeable charging during peak hours (12 PM to 9 PM), specifically from 6 PM to 8:30 PM. Charging during shoulder-load hours is also observed.

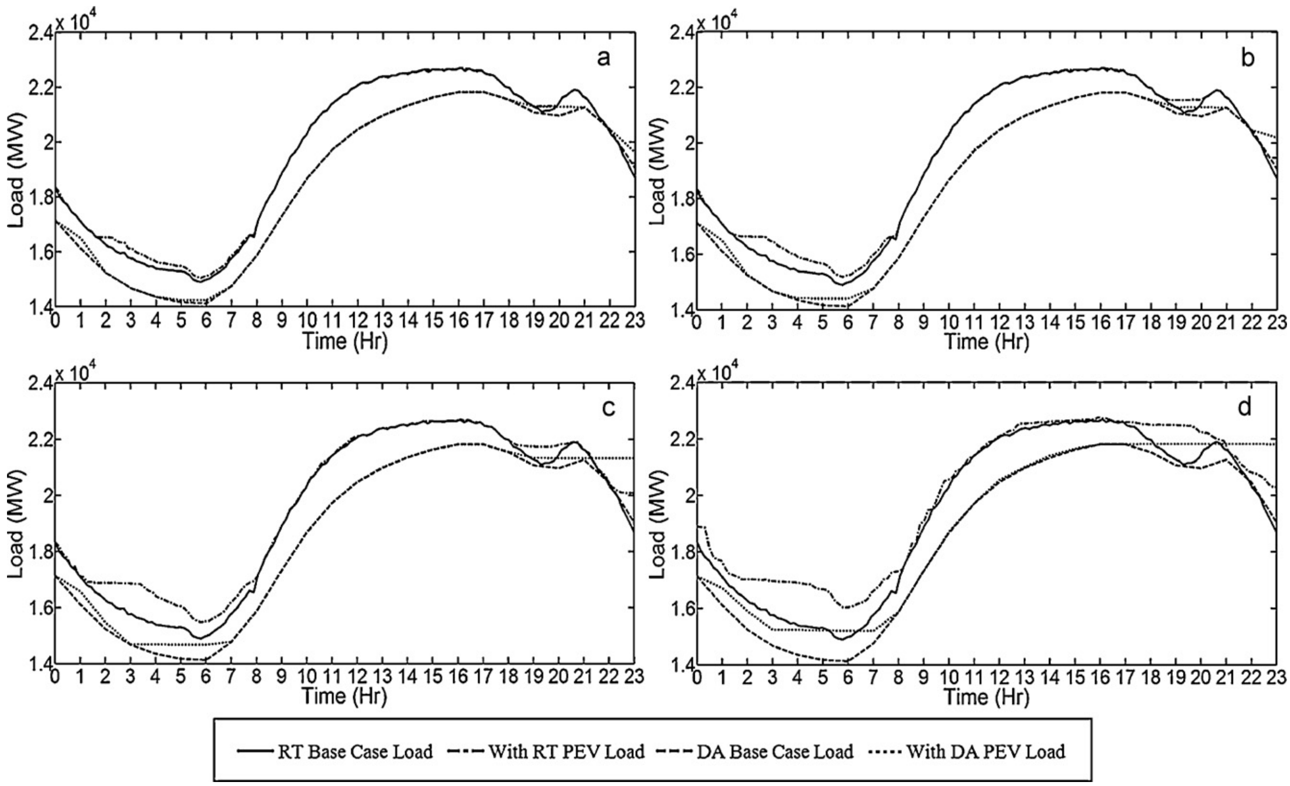

Fig. 4. Day-ahead (DA) and real-time (RT) load profiles with intelligent PEV charging for July 9th with a 70/30 (Level 1/Level 2) charger mixture. PEV penetrations: (a) 5%, (b) 10%, (c) 20% and (d) 40%.

6.2. Intelligent charging vs. valley-filling

Fundamentally, the intelligent charging model optimizes the combined system benefit of charging at periods of low base load and charging to reduce system ramping. This principle is clearly demonstrated in Fig. 4, where the base load ramps down and then up again by roughly 1 GW over 2.5 h in the late evening, creating a second load peak. The cost of rapidly changing generator set points can be high – $50–$400 per ramp operation depending on the generator type [27]. Consequently, the system can encourage PEV charging at this time to fill this second valley and smooth the overall load profile.

While smoothing takes place even at the lowest PEV penetrations, the true utility of this dispatchable load is evident only with a larger number of vehicles. At 20% PEV penetration, the second peak is effectively eliminated, and at 40% the peak is further smoothed to create the familiar concave load shape from 8 AM to 11 PM.

Specifically for July 9th, Table 3 tabulates the relative percentages of energy charged at valley-, shoulder-, and peak-load hours, where

$$\text{PEV charge percentage} = \frac{\text{amount of energy charged at period}}{\text{daily PEV energy requirement}} \times 100 \qquad (22)$$

Table 3
Charging at valley, shoulder, and peak hours for July 9th 2006.

PEV penetration (%)	Real-time		
	Valley charge (%)	Peak charge (%)	Shoulder charge (%)
July 9th (70/30 charger mix)			
5	77.6	11.6	10.8
10	74.8	15.4	9.8
20	70.3	14.3	15.4
40	55.6	24.0	20.4

Table 3 illustrates that for July 9th, there is significant charging at peak-load hours averaging from 11.6% for 5% PEV penetration to 24.0% for 40% PEV penetration. Charging at shoulder is approximately equal to that at peak-load. Overall, charging at non-valley-load hours account for about 1/2 of the total daily charge. Peak-load charging percentage increases across the four PEV penetrations. The corresponding load profiles show that the peak-load is dramatically smoothed at 40% PEV penetration. Moreover, the valley-load dip at 6 AM remains with all four PEV penetrations. Subsequent analysis shows that this dip is due to a base-case load dip and the 70/30 charging constraint.

Table 4
Average vehicle charging at valley, shoulder, and peak hours for June, July, and August 2006.

PEV penetration (%)	Real-time		
	Valley charge (%)	Peak charge (%)	Shoulder charge (%)
June avg. (70/30 charger mix)			
5	79.2	10.5	10.4
10	80.3	10.4	9.3
20	81.0	7.9	11.2
40	73.0	12.6	14.4
Average	78.4	10.3	11.3
July avg. (70/30 charger mix)			
5	77.9	9.8	12.3
10	82.2	7.8	10.0
20	81.7	5.5	12.8
40	73.5	9.9	16.6
Average	78.8	8.3	12.9
August avg. (70/30 charger mix)			
5	78.0	11.1	10.9
10	79.4	11.0	9.6
20	78.4	9.8	11.8
40	69.9	13.5	16.6
Average	76.4	11.4	12.2

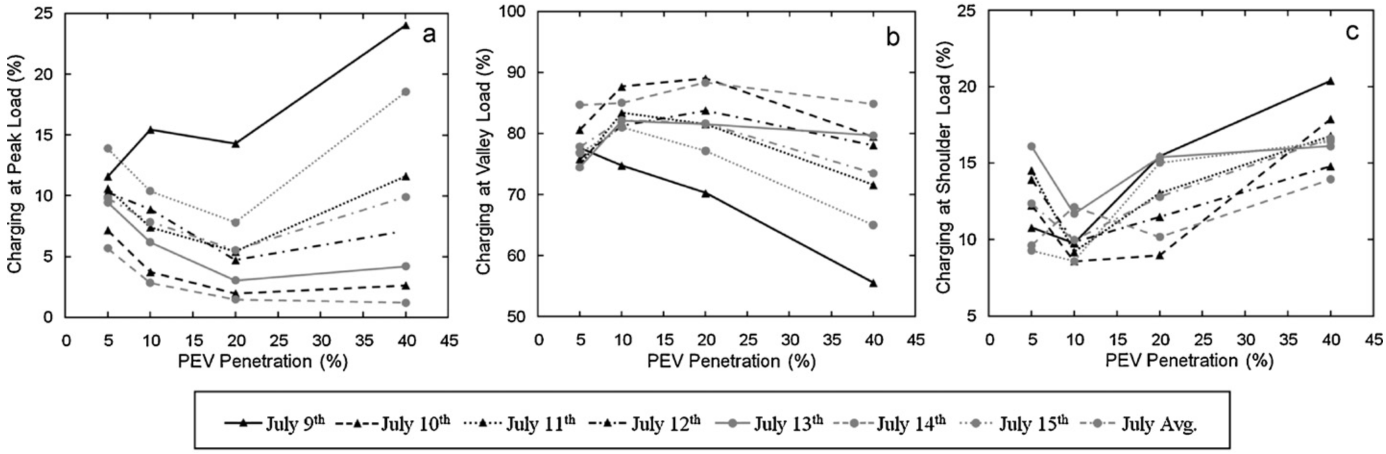

Fig. 5. Percentage of intelligent charging at: (a) peak-load hours, (b) valley-load hours, and (c) shoulder-load hours for July 9th to 15th.

Given the 70/30 ratio of Level 1/Level 2 chargers, average charging percentages for all four PEV penetrations has similar average trends for the three months. Namely, 76.4–78.8% of charging is done at valley-load hours, 8.3–11.4% at peak-load hours and 11.3–12.9% at load shoulder-load hours.

Table 4 tabulates the average charging percentages for the month of June, July and August. On average, charging at valley-load hours is 3.5 times charging at non-valley-load hours. For all three months there is decreased average marginal incentive to charge at valley-load hours at 40% PEV penetration compared to lesser penetrations. In an optimal charging scenario, there are competing incentives for scheduling at both valley and non-valley hours: during valley hours the steady-state cost of energy is low, however there is less benefit in terms of ramping reduction due to the $\bar{P}|\overline{\Delta P}|$ term in Eq. (6); conversely at non-valley hours, there is a larger benefit to ramping reduction, but it is offset by higher steady-state cost.

While the exact charging percentages vary from day to day, the general trend for charging at valley- and shoulder-load hours for the four PEV penetrations is clear. At low to medium PEV penetrations (5–10%), the marginal benefit of increasing charge at valley-load hours to take advantage of low steady-state base case load is higher than the marginal benefit of charging at non-valley-load hours to lower system ramping cost. The marginal benefit of charging at valley and non-valley hours is balanced at a medium to high PEV penetrations (10–20%). At high PEV penetrations (20–40%) there is decreased marginal economic incentive to charge at valley-load hours as the valley becomes smooth. Conversely, there is increased marginal incentive to reduce high system ramping costs at non-valley-load hours. This motivation is illustrated in Fig. 5.

Fig. 5 illustrates that (with the exception of July 9th) there is a benefit to charging at valley-load hours for low to medium PEV penetrations. However at high PEV penetration, there is not a clear trend for charging at peak. A close inspection of the load profiles shows that different days (e.g. July 14th and 15th) have drastically different base case peak-loads. July 14th is a day where load at peak follow a smooth sinusoidal profile, requiring little PEV charge allocation for system ramp smoothing. However, July 15th has significant peak-load “dips”, requiring PEV allocation at peak-load hours to decrease system ramping cost. Consequently, different base case load shapes are the primary cause for the lack of a clear trend for high penetration PEV charge allocation at peak-load hours.

The intelligent charging results from the 21 days are categorized as: maximum charging at peak-load hours, maximum charging at valley-load hours, and typical charging. In Fig. 6, July 9th is one of the maximum peak charging scenarios. System cost reductions due to intelligent PEV charging and a flat valley-fill approach is based off unregulated charging, which will occur without retail electricity price penalties, grid reliability constraints or instituted policy.

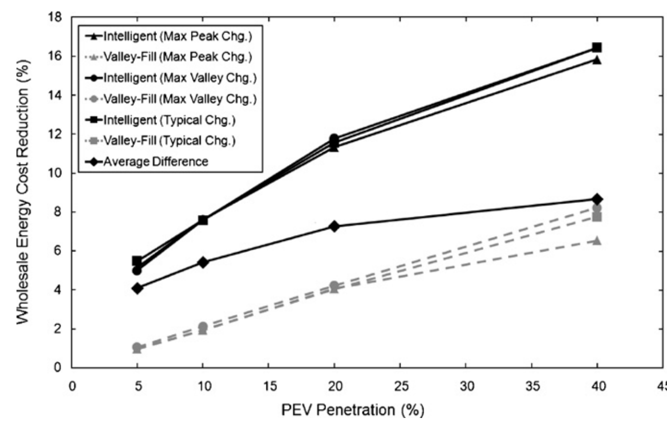

Fig. 6. Wholesale energy cost reductions due to intelligent and valley-fill PEV charging with 70/30 (Level 1/Level 2) charger mixture for three charging results: maximum charging at peak, at valley and typical charging.

Fig. 6 demonstrates that an intelligently charged PEV fleet that is charged mostly at valley-load, with some charging at shoulder and peak-load, reduces system cost from 5% at 5% PEV penetration to 17% at 40% PEV penetration. In comparison, a flat valley-fill charging scheme reduces system cost 1–8%; 4–9% less than intelligent charging.

6.3. Impact of the Charge Flexibility Constraint

Independent of cost modeling, the Charge Flexibility Constraint (CFC) has a significant impact on the dispatch of PEV charging demand, particularly in the morning load valley period. Installing 50% Level 2 chargers relaxes this constraint; however the system benefit of adding these high power charging stations diminished rapidly.

Fig. 7 shows that charging at valley hours from 2 AM to 6 AM increases as more Level 2 chargers are used. This trend is demonstrated with Level 2 charger percentages from 30%, to 50 to 70%. The CFC for the 70/30 (Level 1/Level 2) charger mix prohibits any additional PEV charging between hours 2 AM to 6 AM. This constraint prohibits a flat valley-fill. The CFC is greatly alleviated with a 50/50 charger mix, and the valley-load becomes flatter. With a significant Level 2 charger investment resulting in a 30/70 charger

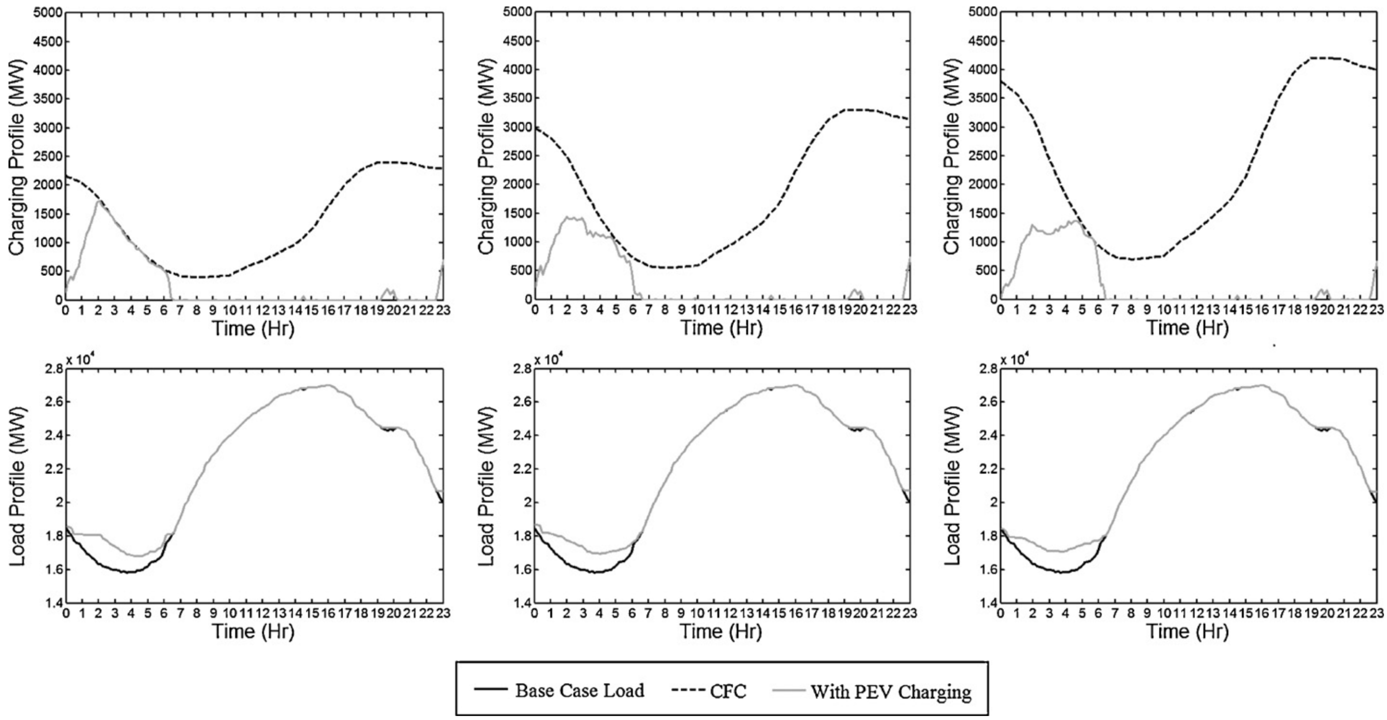

Fig. 7. Effect of the Charge Flexibility Constraint (CFC) on the intelligent charging of 20% PEVs with Level 1/Level 2 charger mixtures: (left) 70/30, (middle) 50/50 and (right) 30/70.

mix, the charging constraint is mostly eliminated, except from 5 AM to 6 AM. This allocation reduces ramping cost at valley-load while taking advantage of the low steady-state load and price at those hours.

The slight valley-load dip from 2 AM to 5 AM is never completely eliminated. An inspection of the CFC indicates that the constraint is inactive between these hours. Instead the cause of such a slight dip is economic. Instead of completely smoothing valley-load, PEV is marginally allocated at the peak-load hours of 7 PM and 8 PM, and shoulder-load hours of 10:30 PM to 11 PM. This is because the marginal economic benefit of completely flattening valley-load is less than that for allocating the remaining PEV load at the indicated hours. Furthermore, at 4 AM to 5 AM the constraint is still active forcing the dip in load. Consequently, at 2 AM and 3 AM PEV charging is also slightly curtailed to allow for smoother ramping once the CFC becomes active.

As the valley-load timing can significantly change the PEV allocation (particularly with large market penetrations) the importance of accurate load forecasting becomes clear. If forecast misses the timing of the valley-load, then there can be a noticeable error in the commitment of the generators and PEV allocation. Such circumstances would create additional system inefficiencies from over- or under-commitment. This phenomenon is shown in Fig. 8.

This charging constraint can place severe limitations on any valley-filling approach when the valley-load hours are centered on 5 AM. However, due to a sharp decrease in maximum charging from 1 AM to 6 AM, a valley-load shift of 1–3 h to the left can significantly diminish the effect of the CFC.

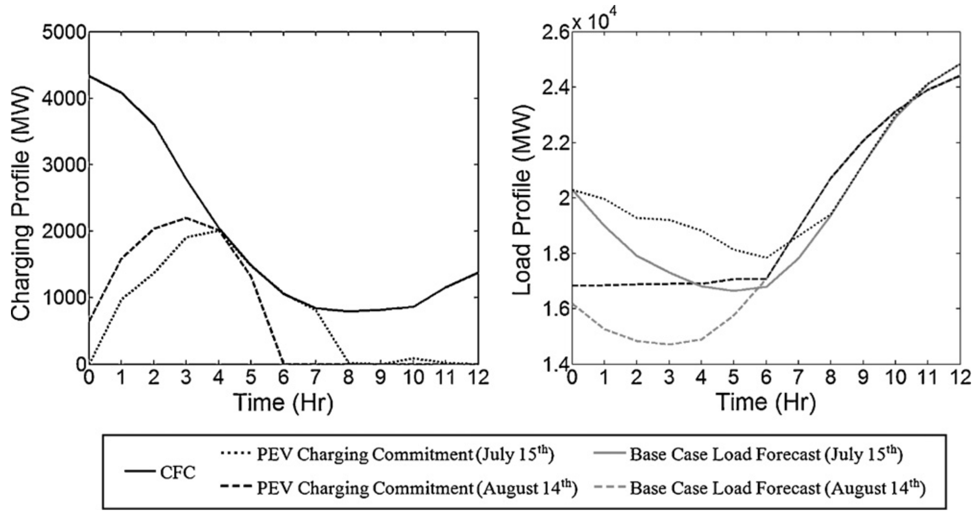

Fig. 8. Effect of base case load forecast and the Charge Flexibility Constraint (CFC) on day-ahead PEV charging commitment in the load-valley for July 15th and August 14th.

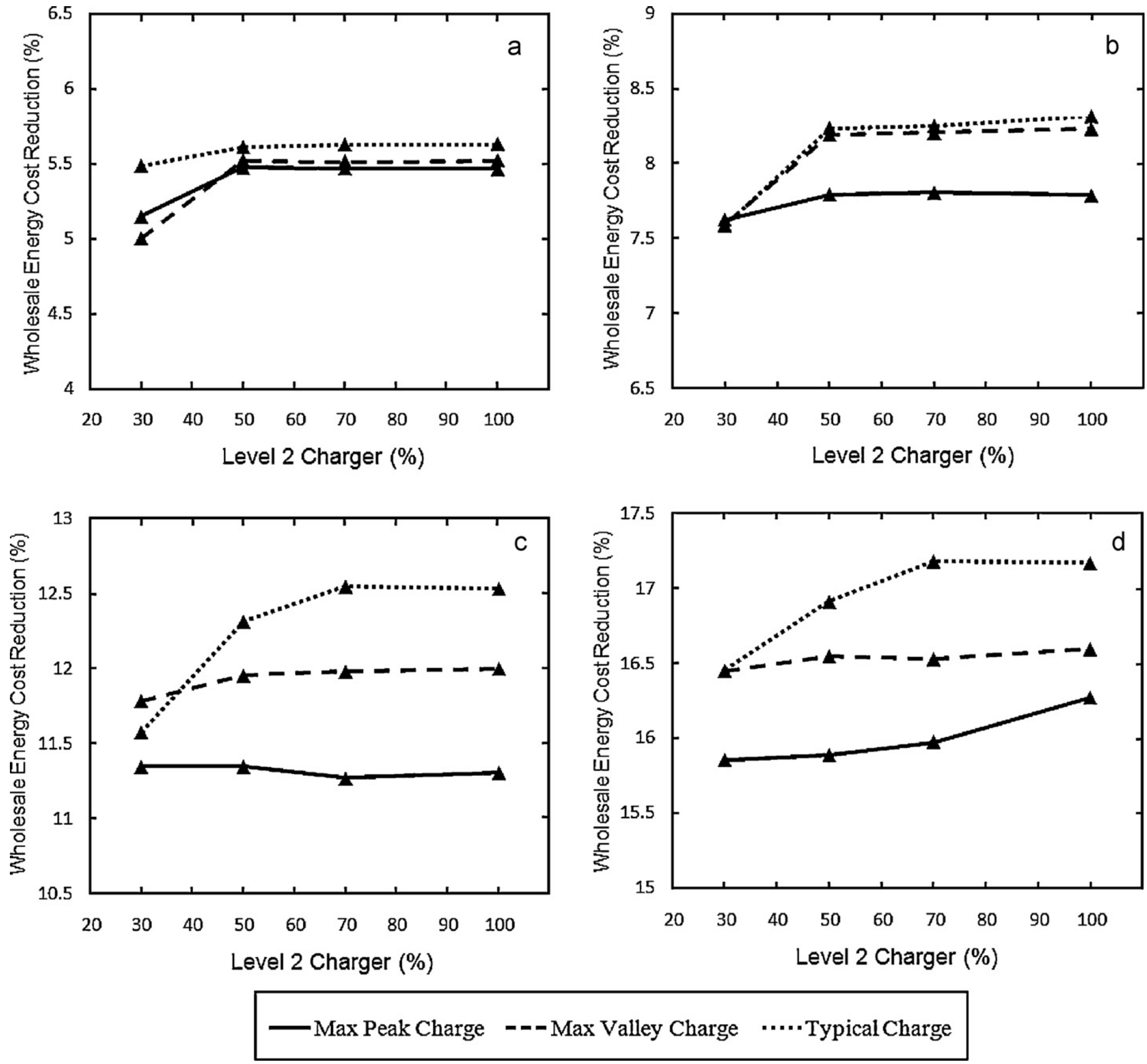

Fig. 9. Effect of Level 2 charger penetration on wholesale energy cost for three charging results: maximum charging at peak, at valley and typical charging. PEV penetrations: (a) 5%, (b) 10%, (c) 20% and (d) 40%.

It is worth noting that Fig. 7 shows that there is a minute amount of PEV charging at the end hour. This is a solver limitation. Because this study only analyzed a daily load pattern rather than a longer time frame, the model attempts to smooth the ramping down at the end hour without connecting to the next day. If the connection is made, then there will be a slightly smoother valley-load, and slightly less PEV allocation at the end hour.

6.4. Impacts of adding Level 2 chargers

The normalized unregulated charging profile in Fig. 1 is constructed with a 70/30 charger mixture. With higher Level 2 charger penetration, the problem of PEV charging at peak load will be exacerbated, resulting in a quadratic increase in LMP and cubic increase in wholesale energy cost.

Fig. 9 shows wholesale energy market cost reductions from intelligently charged PEVs with Level 2 charger penetrations at and above 30%, with the same three charging categories as in Fig. 6. Fig. 9 shows that at low to medium PEV penetrations (5%-10%) increasing the infrastructure investment from 30% to 50% Level 2 chargers reduces wholesale electricity cost by 0.40% on average. However, at medium to high PEV penetrations (20–40%), this investment only reduces cost by 0.25% on average. Further investment to increase the share of Level 2 chargers from 50% to 70% or from 50% to 100% would on average reduce system cost less than or equal to 0.11% or 0.15%, respectively.

Overall, the system benefit is significantly reduced for more than 50% penetration of Level 2 chargers due to the decreased effect of the CFC on PEV charging in the morning valley load hours. This reduction in benefit is exacerbated by a decrease in the percentage of valley charging for higher PEV penetrations as illustrated in Fig. 5. Moreover, as more PEVs charge at peak- and shoulder-load hours, the difference between the optimal charge profile and the unregulated charge profile decreases. From the perspective of only regulating PEV charging, the additional cost of investing in Level 2 chargers above the 50/50 mixture may outweigh the benefit in reducing system cost.

It is worth noting that in Fig. 9 the reduction in system cost is relative to a fixed unregulated charging profile with a 70/30 charger mixture. This value, the lowest considered in this study, was selected to provide a benchmark for the system benefit of adding additional high power charging stations.

7. Conclusions

As Plug-in Electric Vehicle (PEV) ownership grows, controlling when these vehicles charge becomes an important issue for energy providers. Perhaps the most well-known regulated charging policy is the so-called valley-fill where vehicle charging takes place only in the early morning when system demand is lowest.

Motivated to improve upon the valley-filling method, this study considers PEV market penetrations of 5%, 10%, 20%, and 40% in New York State, participating in the New York Independent System Operator's day-ahead and real-time energy markets. For 21 days in June, July and August of 2006, vehicle scheduling decisions are made using a statistical Locational Marginal Price (LMP) and wholesale energy cost model that explicitly includes the dynamic cost of generator ramping in addition to the traditional steady-state operation model. This model creates a framework with two competing cost objectives.

This study also proposes a Charge Flexibility Constraint (CFC) modeling commuter driving behavior and the investment in Level 1 (1.44 kW) and Level 2 (7.68 kW) charging infrastructure. The CFC, which is independent of market modeling, severely restricts PEV charging, particularly in the morning load valley hours. As a result, a complete valley-filling in the New York Control Area cannot be achieved for most charger mixtures. Using a Simulated Annealing optimization algorithm, the proposed intelligent PEV charging method, which minimizes cost from both steady-state and ramping operations, is shown to reduce wholesale energy cost 4–9% beyond that of the valley-fill scheme.

Adding more Level 2 chargers without regulating PEV charging will significantly increase LMP and wholesale energy cost due to increased unregulated charging at peak load. The proposed intelligent PEV charging method will lead to a noticeable reduction in system cost if the penetration of Level 2 chargers is increased from 70/30 to 50/50 (Level 1/Level 2) mixture. However, the system benefit is drastically decreased for higher penetrations of Level 2 chargers due to the diminished effect of CFC on PEV charging in the morning. This trend is exacerbated by a smaller percentage of charging at valley load hours for high PEV penetrations.

Acknowledgements

We would like to thank Tim Mount, Lindsay Anderson, Ray Zimmerman and Robert Thomas at Cornell University for their feedback. This paper was prepared with the support of the U.S. Department of Energy for "The Future Grid to Enable Sustainable Energy Systems," an initiative of the Power Systems Engineering Research Center which is an NSF Industry/University Cooperative Research Center.

References

[1] M.H. Albadi, E.F. El-Saadany, Electric Power Systems Research 78 (November (11)) (2008) 1989–1996, doi:10.1016/j.epsr.2008.04.002, ISSN 0378-7796.
[2] R.N. Boisvert, P.A. Cappers, B. Neenan, The Electricity Journal 15 (April (3)) (2002) 41–51, doi:10.1016/S1040-6190(02)00277-4, ISSN 1040-6190.
[3] A. Brooks, E. Lu, D. Reicher, C. Spirakis, B. Weihl, IEEE Power and Energy Magazine 8 (May–June (3)) (2010) 20–29, doi:10.1109/MPE.2010.936349.
[4] A. Papavasiliou, S.S. Oren, in: IEEE Energy 2030 Conference, 17–18 November, Energy (2008) 1–7, doi:10.1109/ENERGY.2008.4781058.
[5] G. Keith, B. Biewald, D. White, Synapse Energy Economics (prepared for US EPA), 2003.
[6] B.K. Purushothaman, U. Landau, Journal of Electrochemical Society 153 (A533) (2006), doi:10.1149/1.2161580.
[7] J. Li, E. Murphy, J. Winnick, P.A. Kohl, Journal of Power Sources 102 (December (1–2)) (2001) 302–309, doi:10.1016/S0378-7753(01)00820-5, ISSN 0378-7753.
[8] P. Denholm, W. Short, An Evaluation of Utility System Impacts and Benefits of Optimally Dispatched Plug-in Hybrid Electric Vehicles [NREL], 2006.
[9] The Massachusetts Division of Energy Resources, Installation Guide for Electric Vehicle Charging Equipment, 2000.
[10] P. Mohseni, R.G. Stevie, IEEE Power & Energy Society General Meeting, PES'09, 26–30 July, 2009, pp. 1–5, doi:10.1109/PES.2009.5275921.
[11] K. Parks, P. Denholm, T. Markel, Costs and Emissions Associated with Plug-in Hybrid Electric Vehicle Charging in the Xcel Energy Colorado Service Territory [NREL], 2007.
[12] K. Valentine, J. Acquaviva, E.J. Foster, K. Max Zhang, Journal of Power Sources 196 (March (6)) (2011) 3378–3386, doi:10.1016/j.jpowsour.2010.11.110, ISSN 0378-7753.
[13] J. Axsen, K.S. Kurani, The Early U.S. Market for PHEVs: Anticipating Consumer Awareness, Recharge Potential, Design Priorities and Energy Impacts, Institute of Transportation Studies, University of California, Davis, Research Report UCD-ITS-RR-08-22, 2008.
[14] US Census, Summary File 3, 2000, http://factfinder.census.gov/jsp/saff/SAFFInfo.jsp?_lang=en&_sse=on&_content=sp4_decennial_sf3.html&_title=Summary+File+3+%28SF+3%29.
[15] E.H. Allen, J.H. Lang, M.D. Ilic, IEEE Transactions on Power Systems (2008).
[16] U.S. Department of Energy, Transportation Energy Data Book, 29th edition, http://www-cta.ornl.gov/data/index.shtml.
[17] National Congestion Tables, http://mobility.tamu.edu/ums/congestion_data/tables/national/table_1.pdf.
[18] New York City Department of City Planning, Population Division, Journey to Work Tables, 2008, http://home2.nyc.gov/html/dcp/html/census/journey tables.shtml.
[19] Parsons Brinckerhoff Quade Douglas Inc., General Final Report, 2000, http://www.nymtc.org/project/surveys/files/fr00321.pdf.
[20] NYISO Market Information Page, http://www.nyiso.com/public/about_nyiso/understanding_the_markets/energy_market/index.jsp.
[21] M. Tanaka, Energy Policy 34 (December (18)) (2006) 3634–3643, doi:10.1016/j.enpol.2005.07.012, ISSN 0301-4215.
[22] T. Mount, A.J. Lamadrid, IEEE Power and Energy Society General Meeting, 25–29 July, 2010, pp. 1–9.
[23] R.D. Zimmerman, C.E. Murillo-Sánchez, R.J. Thomas, IEEE Power and Energy Society General Meeting, 26–30 July, 2009, pp. 1–7.
[24] N. Deeb, IEEE International Conference on Systems, Man and Cybernetics, vol. 2, 18–21 October, 1992, pp. 1086–1089, doi:10.1109/ICSMC.1992.271645.
[25] A. Viana, J.P. de Sousa, M. Matos, IEEE Porto Power Tech. Proceedings, vol. 2, 2001, doi:10.1109/PTC.2001.964747, 4 pp.
[26] M. Basu, International Journal of Electrical Power & Energy Systems 27 (February (2)) (2005) 147–153, doi:10.1016/j.ijepes.2004.09.004, ISSN 0142-0615.
[27] C. Wang, S.M. Shahidehpour, IEEE Transactions on Power Systems 10 (February) (1995) 60–67.